J Bioenerg Biomembr (2011) 43:437–446
DOI 10.1007/s10863-011-9370-7

MINI-REVIEW

Photosynthetic water oxidation vs. mitochondrial oxygen reduction: distinct mechanistic parallels

Todd P. Silverstein

Published online: 16 July 2011

Abstract The photosynthetic oxygen evolving complex (PSII-OEC) and the mitochondrial cytochrome c oxidase (CcO) not only catalyze anti-parallel reactions (the OEC oxidizes water to dioxygen, whereas CcO reduces dioxygen to water), they also share a number of uncanny molecular and mechanistic similarities. Both feature a redox-active polymetallic cluster that includes a key tyrosine, and both utilize a two-phase mechanism. In one phase the polymetallic cluster undergoes four sequential one-electron transfers: In the PSII-OEC, four successive photooxidations of the photosystem II reaction center P680 (to $P680^{+}$) allows acceptance of 4×1e- from the Mn_4Ca cluster; in CcO, four reduced cytochrome c Fe^{2+} cations donate 4×1e- to the bimetallic center. In the second phase for each enzyme, the polymetallic cluster undergoes a single four-electron transfer with the O_2/2 H_2O redox couple. Intriguing mechanistic similarities between these two complex redox enzymes first delineated over a decade ago by Hoganson/Proshlyakov/Babcock et al. are updated and expanded in this article.

Keywords Cytochrome c oxidase · Complex IV · Oxygen evolving complex · Water oxidizing complex

Introduction

It has been known for several decades that the oxygen evolving complex of photosystem II (PSII-OEC) and the mitochondrial cytochrome c oxidase (Complex IV, or CcO) catalyze anti-parallel reactions: The PSII-OEC oxidizes water to dioxygen, whereas CcO reduces dioxygen to water. These two complex proteins are distinct on a number of levels. CcO is a mitochondrial inner membrane integral protein that serves as a redox-driven proton pump. In this reaction,

$$4Fe_c^{2+} + O_2 + 8H_i^{+} \rightarrow 4Fe_c^{3+} + 2H_2O + 4H_o^{+}$$

four substrate protons from the matrix ($4H_i^{+}$) are incorporated into the 2 H_2O products. The free energy from the spontaneous redox reaction ($\Delta G^{\circ\prime}$ = +0.580 eV (0.815–0.235) = −53.5 kcal/mol) is utilized to pump four protons from the matrix to the intermembrane space/cristae lumen ($4H_i^{+} \rightarrow 4H_o^{+}$).

On the other hand, the OEC, part of the chloroplast thylakoid membrane PSII D1 subunit, catalyzes the oxidation of water: After four successive photooxidations of the special pigment in the PSII reaction center (P_{680}), two water molecules are oxidized to dioxygen.

$$4P_{680}^{+} + 2H_2O \rightarrow 4P_{680} + O_2 + 4H_o^{+}$$

Due to the extremely high redox potential of ground state P_{680} (Rappaport et al. 2002), water is oxidized spontaneously by the PSII-OEC: $\Delta G^{\circ\prime}$ = +0.44 eV (1.26–0.815) = −41 kcal/mol. The OEC is exposed only to the outer, lumenal phase, to which it releases four protons during water oxidation; because it does not take up protons from the inner, stromal phase, it is not a proton pump. The OEC portion of PSII passes electrons from water to $P680^{+}$, but PSII as a whole is a light-driven water/plastoquinone oxidoreductase. Although both the OEC and CcO are metalloproteins, CcO is a heme-copper oxidase, whereas the OEC is a manganese-calcium oxidase.

Besides these differences, Hoganson, Proshlyakov, Pressler and Babcock (1998; Proshlyakov et al. 1998)

T. P. Silverstein (✉)
Chemistry Department, Willamette University,
Salem, OR 97301, USA
e-mail: tsilvers@willamette.edu
URL: http://willamette.willamette.edu/cla/chem/faculty/silverstein/index.php

pointed out over a decade ago a number of uncanny similarities between these non-homologous metalloproteins. Both contain a polymetallic cluster that serves as a four-electron charge accumulator. This cluster gains (CcO) or loses (OEC) four electrons, one at a time, via a one-electron "wire." Once the polymetallic cluster changes oxidation state by four, the O_2/2 H_2O redox conversion is carried out. In CcO, a bimetallic center containing cytochrome a_3, Cu_B and a tyrosine catalyzes four-electron oxygen reduction; electrons are then carried from the one-electron donor cytochrome *c* ($Fe_c^{2+/3+}$) into the bimetallic center via $Cu_A^{2+/1+}$ and cytochrome *a* ($Fe_a^{3+/2+}$). The PSII-OEC contains a pentametallic Mn_4Ca cluster, within which three of the Mn cations undergo oxidation state changes during the photocycle, leading to the four-electron oxidation of 2 H_2O to O_2. Electrons are carried from the Mn_4Ca cluster to the one-electron acceptor $P680^+$ via a special tyrosine. Both enzymes contain a redox-active tyrosine (Y) that shuttles between the reduced phenol tyr-OH and the oxidized phenoxy radical tyr-O·: Y_{288} in CcO and Y_Z in the OEC. Furthermore, both of these special tyrosines maintain close contact with a nearby critical histidine imidazole group: $histidine_{190}$ in the OEC (Rappaport and Lavergne 1997; Ahlbrink et al. 1998; Hays et al. 1998; Mamedov et al. 1998), and $histidine_{284}$ in CcO (Svensson-Elk et al. 2002)

All of the above knowledge has been in biochemistry textbooks for a decade or more (see for example Berg et al. 2007; Voet et al. 2008). Furthermore, in the mid-1970s it became clear that both enzymes functioned in oscillating four-electron cycles during turnover. Kok described the OEC S_0-S_4 cycle in 1970 (Kok et al. 1970; Joliot and Kok 1975), and in 1977 Wikstrom proposed a redox-driven proton pumping cycle for CcO (Wikstrom 1977). However, it is only over the last decade or so that the detailed mechanisms of these two enzymes have begun to be elucidated. The surprising mechanistic kinship between CcO and the OEC, first described by Hoganson, Proshlyakov, Pressler and Babcock (1998; Proshlyakov et al. 1998), was tentatively added to the CcO pathway nomenclature by Wikstrom and Verkhovsky in 2006. As was pointed out long ago (Babcock et al. 1989; Babcock and Wikström 1992; Babcock 1999), the logic behind this mechanistic kinship is explained by the fact that both enzymes must solve the problem of working with the O_2/2 H_2O four-electron redox couple, while avoiding the intermediate reactive oxygen species (superoxide, $O_2^{\cdot -}$; peroxide, H_2O_2; and the hydroxyl radical, OH·), which are all toxic. This is particularly challenging because the electron wires leading into (CcO) or out of (OEC) the active site metal clusters comprise one-electron carriers only. Hence both enzymes have evolved polymetallic O_2/H_2O active sites that serve as 1e- ➔ 4e-charge accumulators. After four sequential one-electron redox processes, they carry out the four-electron O_2/2 H_2O redox conversion, thus avoiding the creation of toxic reactive oxygen species (Babcock et al. 1989; Babcock and Wikström 1992; Babcock 1999).

Mechanistic parallels between CcO and OEC

What follows is a brief overview of current thinking on the basic mechanisms of these two important enzymes, updating the parallel redox cycle schemes first presented by Hoganson et al. in (1998). Details such as side paths and kinetic sub-steps have been omitted from diagrams. In some cases they are included in footnotes, but in general they lie beyond the scope of this article. Cited references may be consulted for further discussion of such details.

In the PSII-OEC, the process begins with the photooxidation of P680 in the PS II reaction center. Capturing four successive photons yields four $P680^+$, which pull four electrons one at a time from the OEC Mn_4Ca cluster (Fig. 1a), via the redox-active Y_Z(−O·/−OH) intermediary. The net oxidation state of the cluster increases by four, from $S_0 = Mn(III)_3Mn(IV)/Y_Z - OH$ to $S_4 = Mn(IV)_4/Y_z - O\cdot$ (Clausen and Junge 2004; Haumann et al. 2005; McEvoy and Brudvig 2004; Howard et al. 2005; Dau and Haumann 2006; Dau and Haumann 2008).[1]

The S_4 state is then equipped to pull four electrons from two water molecules bound to the pentametallic center, oxidizing the 2 H_2O to dioxygen.

In cytochrome c oxidase (Fig. 1b), the reduced bimetallic center in the C_0 (or R) state binds dioxygen and then reduces it in a single four-electron transfer step, giving the C_4 (or P_M) state[2] (Wikstrom and Verkhovsky 2006; Babcock and Wikstrom 1992; Belevich et al. 2006):

$$C_0 = Fe_{a3}(II)/Cu_B(I)/Y_{288} - OH \quad \text{to}$$

$$C_4 = Fe_{a3}(IV){=}O^{2-}/OH^-/Cu_B(II)/Y_{288} - O\cdot$$

Wikstrom and Verkhovsky (2006)

[1] Aside from Y_Z-OH ➔ Y_Z–O· + H^+ + e–, a number of alternative proposals have been put forth regarding the source of the fourth and final electron. Some researchers believe that the S_4 state contains a Mn(V) rather than a Y_Z-O· radical (Clausen and Junge 2004; Haumann et al. 2005). Sproviero et al. (2008) recently proposed that the Y_Z-O· radical in S_4 is re-reduced by a fully deprotonated substrate water (O^{2-}) bound to Mn(IV), yielding the oxyl radical Mn(IV)–$O^{\cdot -}$/Y_Z-OH. This is supported by evidence that absorption of the fourth photon causes an initial deprotonation event, followed by electron removal to $P680^+$, giving the unstable fully oxidized state S_4, which has also been called S_4' (Haumann et al. 2005), and most recently, S_4^+ (Dau and Haumann 2008).

[2] See Appendix I for a brief outline of what happens if CcO begins in the fully reduced state [Cu_A(I)/Fe_a(II)/Fe_{a3}(II)/Cu_B(I)], as opposed to the partially reduced "mixed valence" state [Cu_A(II)/Fe_a(III)/Fe_{a3}(II)/Cu_B(I)] discussed above.

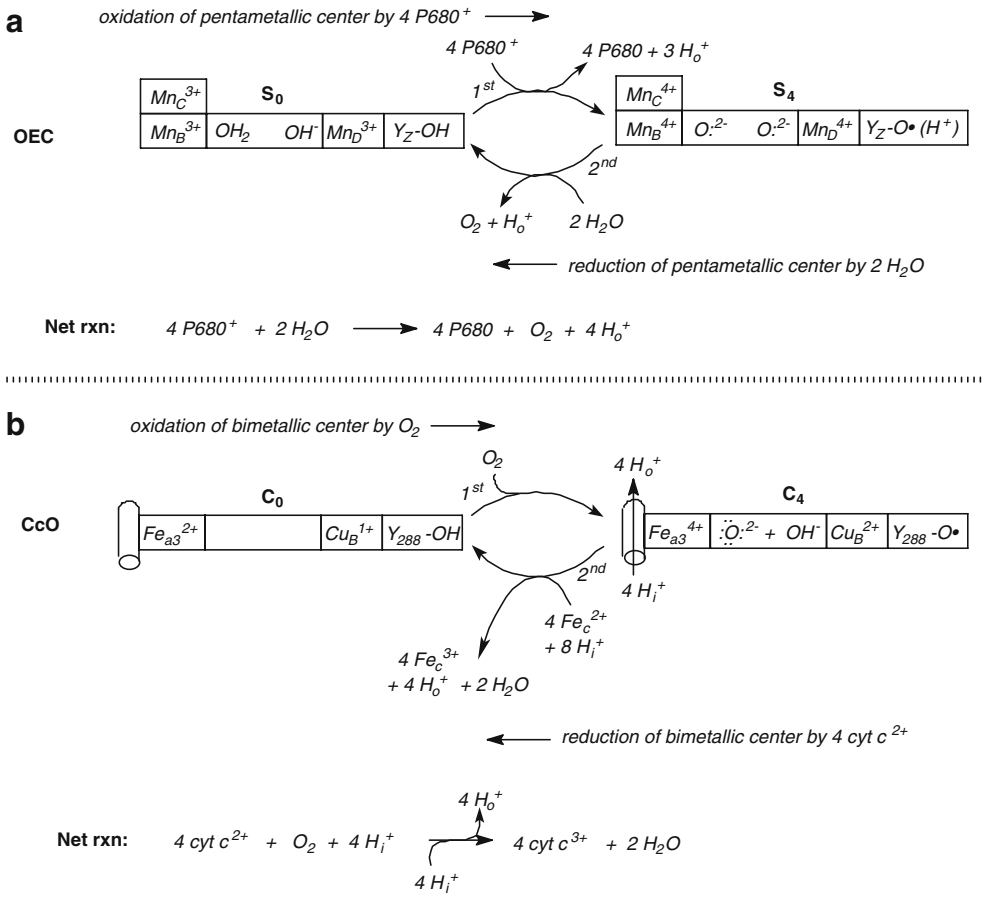

Fig. 1 Comparison of the fully oxidized and reduced polymetallic centers of (**a**) the oxygen evolving complex, and (**b**) cytochrome *c* oxidase. (**a**) The key redox-active components in the OEC active site are three of the four Mn cations, plus tyrosine$_Z$. The remaining Mn and Ca are redox-inactive. Each photosystem II reaction center contains only a single P680 that is oxidized four times by the absorption of four successive photons, along with re-reduction by four successive electrons from the Mn_4Ca center. The initial part of the proton output path may include arginine$_{357}^+$; H_o^+ = proton released into the chloroplast thylakoid lumen (i.e., the outer or external phase (Silverstein et al. 1993)). (**b**) The CcO bimetallic center comprises cytochrome a_3, copper$_B$, plus tyrosine$_{288}$. H_o^+ = proton released into the mitochondrial intermembrane space (i.e., the outer or external phase), and H_i^+ = proton taken up from the mitochondrial matrix (i.e., the internal phase (Silverstein et al. 1993))

In the C_4 state the two oxygen atoms are fully reduced and the bimetallic center is four-electron oxidized. The bimetallic center is then reduced from C_4 back to C_0 by four successive one-electron steps. Each step transfers an electron from cytochrome c (Fe_c^{2+}) into the bimetallic center, via $Cu_A^{(2+/1+)}$ and cytochrome *a* ($Fe_a^{3+/2+}$). For each one-electron step, three things occur: the oxidation state of the bimetallic center declines by one; a "substrate" proton is taken into the bimetallic center to protonate either Y_{288}-O:$^-$ or one of the two reduced oxygen atoms; and a proton is pumped out of the mitochondrial matrix. Note that for both OEC and CcO, the polymetallic/tyrosine center is used to accumulate four successive one-electron transfers, followed by a single four-electron transfer to the O_2/2 H_2O redox couple (Fig. 1).

Figure 2 is an update and expansion of the key Fig. 1 in Hoganson et al. (1998): Here, parallels between the redox mechanism of the PSII-OEC[3] (Fig. 2a) and CcO (Fig. 2b) are clarified. In both Schemes, the left side shows four successive one-electron transfers out of (OEC, 2a) or into (CcO, 2b) the polymetallic center. For the OEC, these take place proceeding from the top[4] to the bottom of Fig. 2a (left), and for CcO in Fig. 2b (left), the one-electron steps proceed from the bottom to the top. Similarly, the right side of each figure shows two successive two-electron transfers between the polymetallic center and the O_2/2 H_2O couple: bottom to top for OEC, and top to bottom for CcO. In both cases, the peroxide two-electron intermediates ($C_2^\dagger$, $S_2^\dagger$)

[3] A somewhat more detailed structural model of the PSII-OEC redox cycle is presented in Appendix II.

[4] Although the dark resting state of the OEC features only 25% of Mn_4Ca clusters in the fully reduced S_0 state and 75% in the S_1 state, for the sake of comparison with CcO, Fig. 2a starts off with the less stable S_0 state.

are unstable and spectroscopically uncharacterized (but see Clausen and Junge 2004). The existence of these putative peroxide intermediates is controversial (Haumann et al. 2008); even if they do exist, they are present for such a short period of time under normal conditions that the two 2e- steps essentially combine into a single kinetic 4e- step. On the other hand, it is certainly permissible to consider from a thermodynamic perspective the impact of breaking the four-electron process into two two-electron processes, with a peroxide intermediate (Hoganson et al. 1998).

Importance of tyrosine

It is interesting to speculate as to why evolution twice arrived at such a similar solution to the 1e-/4e- dioxygen/water redox problem. Both the OEC and CcO have polymetallic centers that lose a total of three electrons, and a tyrosine that undergoes 1e- oxidation. In both cases as well, the tyrosine helps to mediate the two-electron $HOO:^-$/2 H_2O redox process, and seems to be less involved in the $O_2/HOO:^-$ stage of the reaction. Two potential explanations for this tyrosine/peroxide-water connection spring to mind. First of all, electron exchange between phenol oxygen and peroxide/water oxygens is kinetically fairly facile (Cook and Depatie 1959), especially in the presence of iron (Pignatello 1992; De et al. 2006). Secondly, according to molecular dynamics simulations of PSII-OEC performed by Sproviero et al. (2008), Y_Z-O· in the S_4 state catalyzes the formation of the O-O bond by first removing an electron from a fully deprotonated water (O^{2-}) bound to the Mn_4Ca cluster. In order to do this, the Y_Z-O·/-OH redox potential must be sufficiently high (≈ 1.0 V (Tommos and Babcock 1998)) in order to drive this process. On the other hand, in CcO, Y_{288}-$O:^-$ and Cu_B^{1+} break the O-O bond by donating a pair of electrons to the bound peroxide intermediate. In order to do this, the redox potential of Y_{288} must be sufficiently low for the reaction to proceed spontaneously. At the same time, subsequent re-reduction of the Y_{288}-O· radical must be sufficiently spontaneous in order to drive the first proton pumping step (C_4/P_M ➔ C_3/F), hence the prior O-O bond cleaving step must not be too strongly driven. Proshlyakov et al. (1998) sum up this situation thusly: "The use of a cross-linked tyrosine, which is expected to reduce the potential of the radical only modestly from that of the unmodified residue, looks to be an efficient strategy by which to accomplish this."

A few interesting differences between the PSII-OEC Y_Z and CcO Y_{288} are worth discussing here. Y_Z is generally classified as part of the OEC one-electron "wire" and *not* as part of the pentametallic Mn_4Ca cluster (Dau and Haumann 2008; Hoganson and Babcock 1997). In support of this view, the Y_Z-histidine$_{190}$ interaction in the OEC features a non-covalent Y_Z-OH ··· :*N*≡his$_{190}$ hydrogen bond; upon Y_Z oxidation, the hydroxyl proton simply shifts onto the histidine imidazole N:(Y_Z-O· ···· $^+$HN≡his$_{190}$) until subsequent Y_Z reduction and reprotonation. This proton never leaves the Y_Z/his$_{190}$ pair (Rappaport and Lavergne 1997; Sproviero et al. 2008), and is isolated from the arginine$_{357}$/aspartate$_{61}$ proton wire (McEvoy and Brudvig 2004; Sproviero et al. 2008) connecting the pentametallic Mn_4Ca cluster to the lumenal space.[5] Being part of the one-electron "wire," Y_Z is oxidized and re-reduced in each successive light-driven S-transition; the fourth and final photon absorption in the redox cycle is believed to yield a Y_Z-O· radical that is a key component of the fully oxidized S_4^+ state (McEvoy and Brudvig 2004; Dau and Haumann 2006; Dau and Haumann 2008; Sproviero et al. 2008). On the

Fig. 2 Mechanistic details of the O_2/2 H_2O redox cycles for (**a**) the oxygen evolving complex, (**b**) cytochrome *c* oxidase/mixed valence, (**c**) cytochrome *c* oxidase/fully reduced, and (**d**) alternative oxidase. The left side of each figure shows four successive one-electron transfer steps out of (A) and into (B–C) the polymetallic center; electrons travel one-at-a-time along an electron "wire" comprising (A) $Y_Z^{O\cdot/OH}$/$P680^{+/0}$, and (B/C) cyt $a^{3+/2+}$/$Cu_A^{2+/1+}$/cyt $c^{3+/2+}$. The right side of each figure shows two successive two-electron transfer steps (A) from the O_2/2 H_2O redox couple into the polymetallic center, and (B/C) from the bimetallic center into the O_2/2 H_2O redox couple. Bracketed intermediates marked {$X^\dagger$} are transient, kinetically unstable, and spectroscopically uncharacterized. **a OEC**: adapted from Fig. 4 in McEvoy and Brudvig 2004, Fig. 2 in Howard et al. 2005, Fig. 5 in Dau and Haumann 2008, and Fig. 6 in Sproviero et al. 2008. S_0 features a fully reduced Mn_4Ca cluster; S_1 is one-electron oxidized, S_2 two-electron oxidized, etc. The four-electron oxidized S_4 state has been modeled by some groups with an oxidized Mn(V) instead of the Y_Z-O· radical. **b CcO/mixed valence**: adapted from Fig. 1 in Wikstrom and Verkhovsky 2006. C_0 features a fully reduced bimetallic center; C_1 is one-electron oxidized, C_2 two-electron oxidized, etc. The alternate state names (R, A, P_M, etc.) are those often employed by Wikstrom et al. The scheme here depicts the redox cycle starting from the partially reduced "mixed valence" enzyme, in which the bimetallic center is reduced (Fe_{a3}^{2+}/Cu_B^{1+}) and the electron input "wire" is oxidized (Cu_A^{2+}/Fe_a^{3+}). **c CcO: starting with the fully reduced enzyme** "wire" (Cu_A^{1+}/Fe_a^{2+}), the fourth and final electron removed from the bimetallic center comes from cytochrome *a* rather than from Y_{288}-OH, giving a fully oxidized C_4' state (see Appendix I). This C_4' (or P_R) state is unique; protonation of Cu_B-OH- and reduction of Fe_a^{3+} (along with proton pumping) yields the C_3 state, and the three remaining reduction steps and states are then identical to those in (B) above. **d A model for alternative oxidase**, adapted from Fig. 2 (mechanism III) in Affourtit et al. 2002. Oxidation of the bimetallic center by O2 (right side) closely resembles CcO. The left side, reduction of the bimetallic center by 2 QH_2, differs from CcO: the steps involve two successive 2e- transfers (as opposed to four 1e- transfers), and they do not feature proton pumping

[5] Although Hoganson and Babcock (1997) proposed Y_Z as part of the proton exit pathway to the lumen, and Umena et al's most recent 1.9 Å structure (Umena et al. 2011) shows a putative proton exit path emanating away from Y_Z, experimental evidence currently favors the "rocking" model in which the Y_z proton never leaves this site (Rappaport and Lavergne 1997; McEvoy and Brudvig 2004; Sproviero et al. 2008).

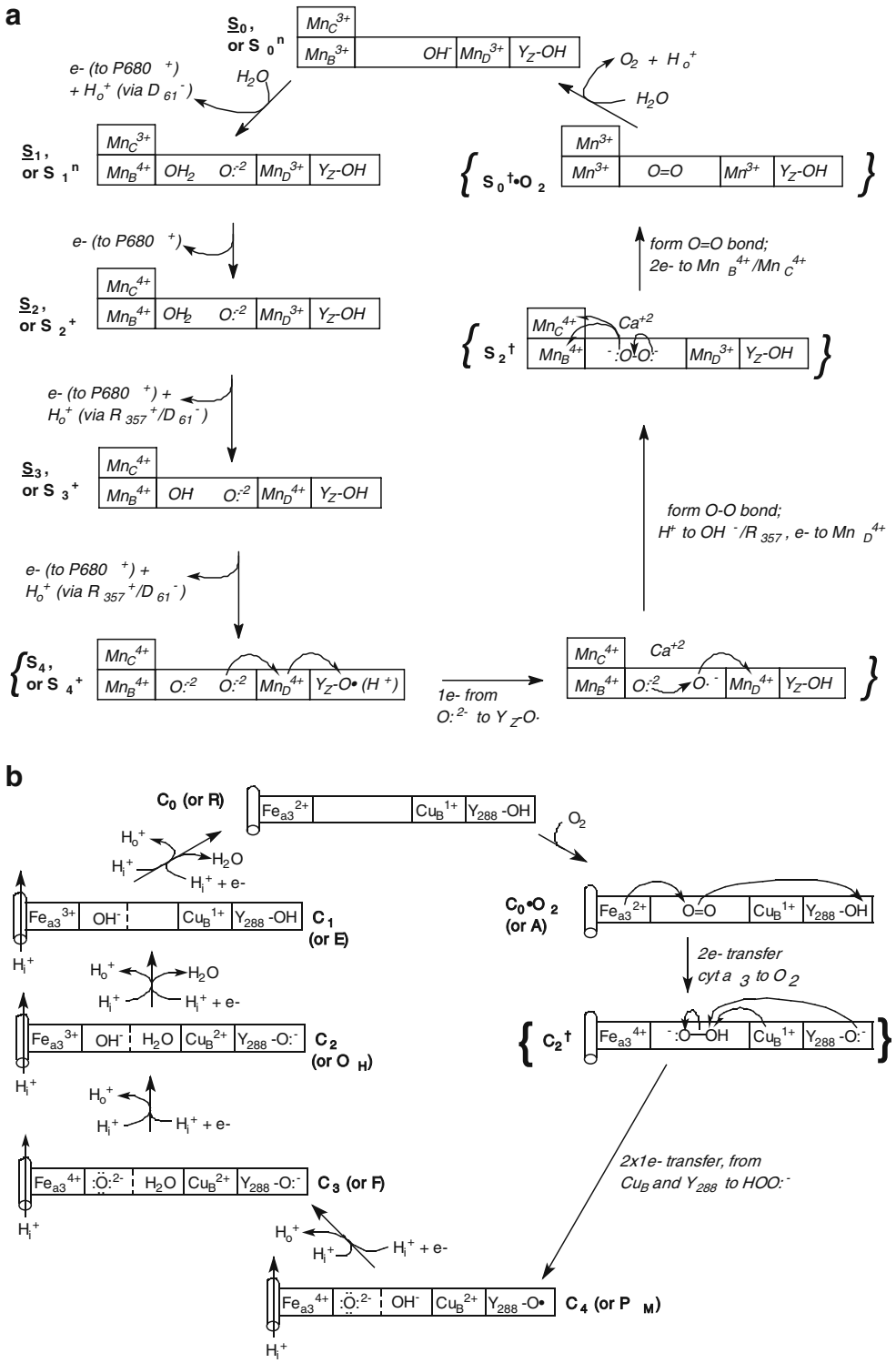

other hand, Y_{288} in CcO differs from Y_Z in the OEC in two key ways: First, Y_{288} is covalently attached to the his_{284} imidazole ring (Svensson-Elk et al. 2002). Second, upon O_2 reduction, both a proton *and* an electron from the tyrosine phenolic OH group are transferred to the substrate dioxygen molecule. In this sense, Y_{288} is considered to be an integral part of the CcO bimetallic center; Y_{288} is oxidized and re-reduced only once, in the $C_2^{\dagger} \rightarrow C_4$ (P_M) $\rightarrow C_3$ (F) portion of the pathway. (When starting from the fully reduced CcO complex, Y_{288} is in fact never oxidized

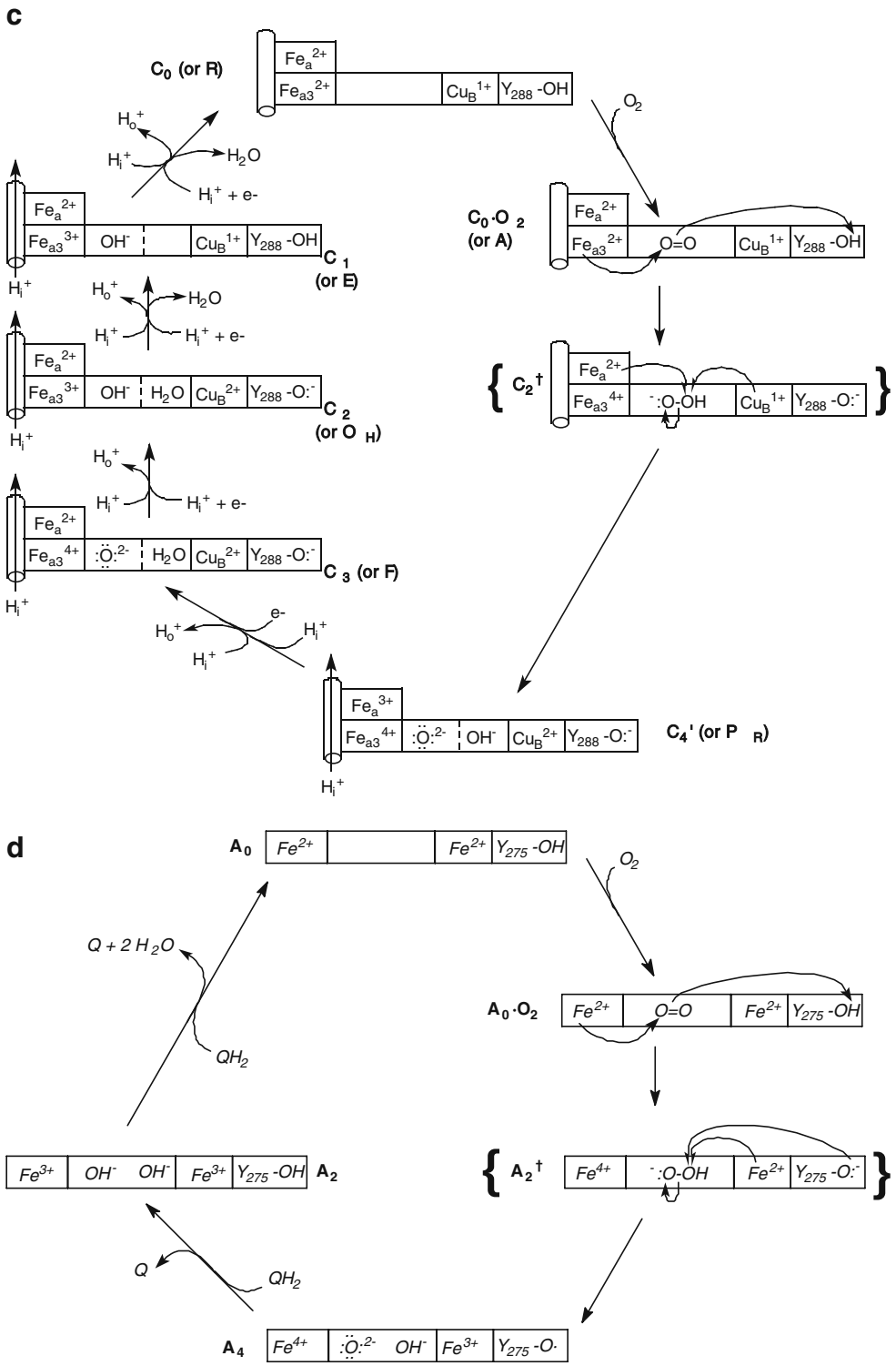

Fig. 2 (Continued)

(Wikstrom and Verkhovsky 2006), as outlined in Fig. 2c and Appendix I.)

Before concluding, it is worth noting that mitochondria in plants and many algae, fungi, and protozoa contain, in addition to CcO, an alternative terminal oxidase (AOx). AOx is a non-heme cyanide-insensitive quinol:dioxygen oxidoreductase that uses a diiron-carboxylate complex to catalyze the reduction of dioxygen to water, by quinol: O_2 + 2 QH_2 ➔ 2 H_2O + 2 Q (Wagner and Moore 1997; Moore et al. 2008). This reaction occurs without any

proton pumping. Several models of dioxygen reduction by AOx feature a tyrosyl phenoxy radical (Affourtit et al. 2002; Marechal et al. 2009); in fact, Y_{275} was recently determined to be in a catalytically active position, within 4 Å of the bimetallic active site (Moore AL 2011, Personal communication, manuscript in preparation). One mechanistic model in particular (Affourtit et al. 2002) mirrors CcO rather closely, as seen in Fig. 2d. In this redox cycle, the diferrous reduced form (A_0) binds dioxygen ($A_0{\cdot}O_2$). Transfer of two electrons yields an unstable ferryl-ferrous bimetallic center with bound peroxide ($A_2^{\dagger}$), which undergoes a further two-electron transfer to give the fully oxidized ferryl-ferric center with tyrosyl radical and bound OH^- + O^{2-} (A_4). Re-reduction of the bimetallic center occurs in two steps: Binding and oxidation of the first quinol yields the two-electron reduced diferric/tyrosine center with two bound hydroxide anions; binding and oxidation of the second quinol returns the bimetallic center to the fully reduced A_0 form, with release of two waters. A comparison to Fig. 2b shows that analogues of these five intermediates are also featured in the CcO redox cycle.

Conclusion

In summary, I have updated and expanded the intriguing structural and mechanistic parallels between water oxidation by the photosynthetic oxygen evolving complex, and oxygen reduction by the mitochondrial cytochrome *c* oxidase, first presented by Hoganson, Proshlyakov, Pressler, and Babcock in 1998 (Proshlyakov et al. 1998). Cognizance of these parallels leads to a number of conclusions. First, applying the Kok S_0-S_4 OEC redox state sequence to CcO yields the C_0-C_4 sequence (Wikstrom and Verkhovsky 2006). This C_0-C_4 redox state nomenclature for CcO is much more informative than the more common alphabetical labels (R, A, P, F, O, E). First of all, the C_0-C_4 subscripts give unambiguous knowledge of the net redox state of the bimetallic center. The alphabetical labels not only lack such information content, they are actually chemically misleading: P stands for peroxy, but the two oxygen atoms in this state are fully reduced and unbonded; F stands for ferryl, but the ferryl Fe^{4+} ion is also found in the earlier P state; O stands for oxidized, but the two earlier F and P states are more oxidized than the O state. For these reasons, adoption of the Kok-Joliot style C_0-C_4 nomenclature for CcO redox states is well-advised.

Lastly, the evolutionary and chemical significance of the OEC/CcO mechanistic parallels are intriguing. Recognition of this could not only bridge the distinct OEC and CcO research communities, it could also help researchers as they craft mechanistic proposals regarding the O_2/2 H_2O redox process. Cognizance of these mechanistic parallels could also guide future projects in the design of more effective chemical and biochemical catalysts for water oxidation.

Appendix I: cytochrome c oxidase in the fully reduced form

The mechanism depicted in Fig. 2b applies to CcO starting out in the "mixed valence" (R) state, in which the electron input groups Cu_A(II) and Fe_a(III) are oxidized while the bimetallic center Fe_{a3}(II) and Cu_B(I) is reduced. If instead, CcO begins in the fully reduced state [Cu_A(I)/Fe_a(II)/Fe_{a3}(II)/Cu_B(I)], then the oxidation proceeds slightly differently (Wikstrom and Verkhovsky 2006) after O_2 binding. Instead of C_4, which features the Y_{288}-O· radical in the fully oxidized form, the final electron is removed from cytochrome *a* in state C_4' (or PR; see Fig. 2c):

$$C_4' = Fe_a(III)/Fe_{a3}(IV){=}O^{2-}/OH^-/Cu_B(II)/Y_{288}{-}O{:}^-$$

The reduction phase then begins by re-reducing cytochrome *a* and protonating Cu_B-OH- to reach state C_3 (or F); this and the remaining states are identical to those in the mixed valence redox cycle (Fig. 2b).

$$C_3' = Fe_a(II)/Fe_{a3}(IV){=}O^{2-}/OH^-/Cu_B(II)/Y_{288}{-}O{:}^-$$

The C_3' state converts to the "normal path" C_3 state by protonation of Y_{288}-$O{:}^-$, coupled to proton pumping.

Appendix II: details of the OEC pentametallic center and redox cycle

Two recent structural studies of the PSII-OEC using EXAFS (Yano et al. 2006) and x-ray crystallography at 1.9 Å resolution (Umena et al. 2011) show the pentametallic $Mn_4CaO_5(H_2O)_4$ cluster to exist in a distorted chair configuration (Fig. 3a). The cubane bottom of the chair includes three Mn, one Ca, and four di-μ-oxo bridges. The square back of the chair includes the fourth Mn (Mn_D from Fig. 3 of Yano et al. 2006); Mn(4) from Fig. 2 of Umena et al. 2011; and one di-H-oxo bridge. Two of the three Mn in the cubane structure are redox active: Mn_B and Mn_C [Mn (1) and Mn(3) from Fig. 2 of Umena et al. 2011] can exist in the +3 or +4 state. Mn_A (Mn(2)) is redox-inactive, existing solely in the +4 state.

The chair is distorted because O(5) (starred in Fig. 3a) has much longer Mn-O bond lengths than all of the other Mn-O bonds (Umena et al. 2011). While Mn-O bonds involving the four di-μ-oxo bridges and the two waters bound to Mn_D average 2.04±0.14 Å, Mn-O(5) bond lengths average 2.5±0.1 Å. Similarly, whereas Ca-O bonds involving both di-μ-oxo bridges as well as two bound waters average

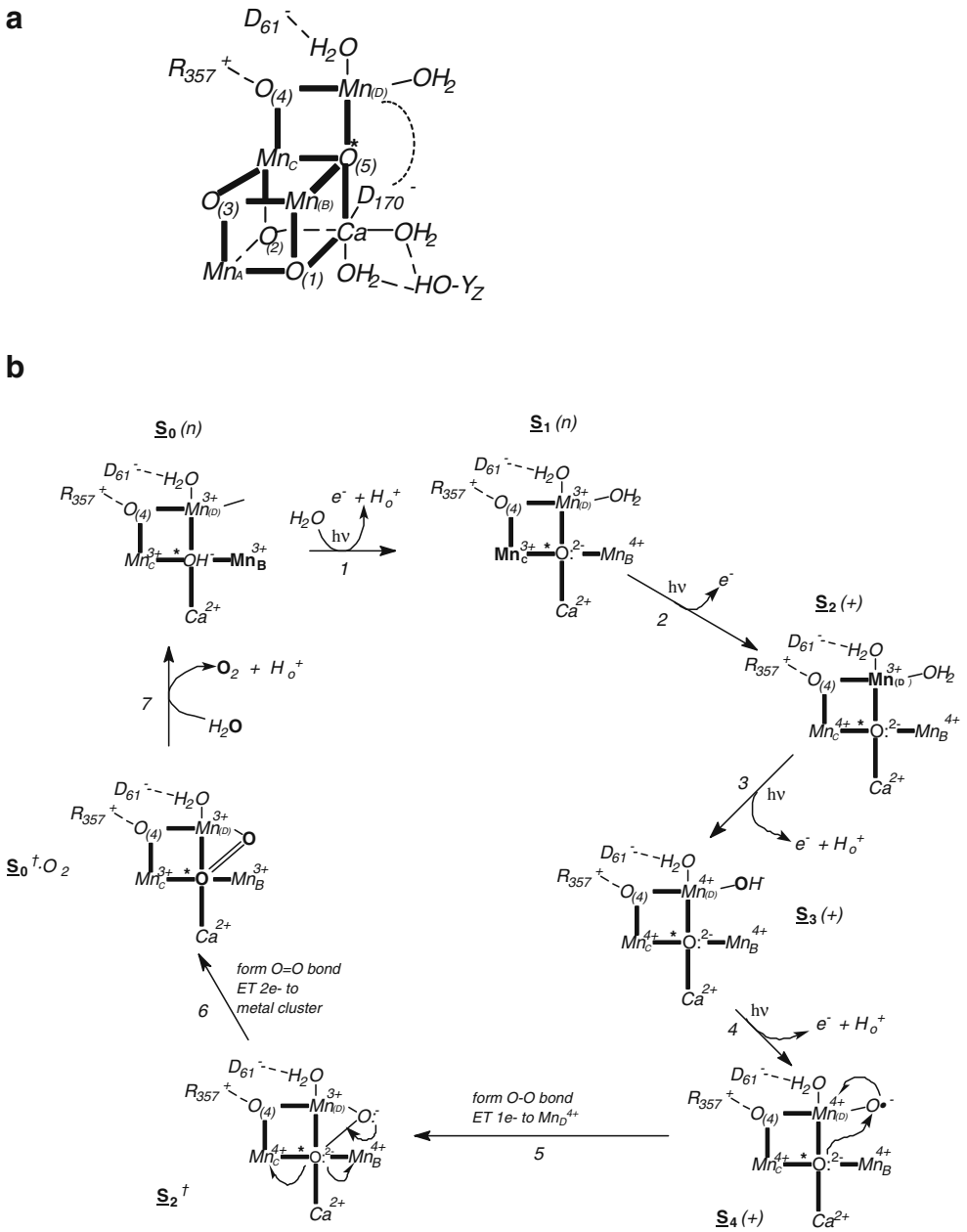

Fig. 3 **a** The "chair" structure of the Mn_4Ca pentametallic cluster, adapted from Figs. 3 and 4 in Yano et al. 2006 and Fig. 2 in Umena et al. 2011. **b** One of a number of proposals outlining the OEC redox cycle. Mn_A in the cubane metallocluster is redox-inactive. Intermediates S_4^+, S_2†, and S_0†·O_2 in the bottom left of the scheme are all unstable and speculative. Adapted from Fig. 4 in McEvoy and Brudvig 2004, Fig. 2 in Howard et al. 2005, Fig. 4 in Yano et al. 2006, Fig. 6 in Sproviero et al. 2008, and Fig. 2 in Umena et al. 2011. A number of mechanistic details of the S_4 to S_0 transition that are omitted from this figure, including the identity and function of the OH^- base catalyst, as well as the catalytic proton transfer functions of arginine-357 and aspartate-61, are discussed in Sproviero et al. 2008

2.43±0.05 Å, the Ca-O(5) bond length is 2.7 Å. Clearly, O(5) makes longer metal-O bonds than all other oxygens in the structure. For this reason, Umena et al. (2011) conclude that O(5) may actually be a hydroxide (OH^-) rather than a bridging oxide (O^{2-}). Furthermore, they hypothesize that the longer bond lengths may allow this oxygen to come and go from the cubane structure, i.e., this OH^- could provide one of the two substrate oxygens to be oxidized to O_2 during the redox cycle. This possibility is depicted in Fig. 3b.

Figure 3b includes only the three redox-active Mn, the distorted O(5) (as a starred OH^-), two waters bound to Mn_D, and the D_{61}^-/R_{357}^+ side-chains implicated in the H^+ efflux pathway (McEvoy and Brudvig 2004; Sproviero et al. 2008).

In the first photooxidation step, Mn_B is oxidized, O(5) loses its proton, and a second water is bound to Mn_D. H^+ efflux presumably occurs by proton hopping through the H_2O-D_{61}^- pair and/or the O(4)-R_{357}^+ pair, and from there through a channel out to the lumen. The second photooxidation removes an electron from Mn_C, and the third from Mn_D; the third step also removes a proton from the substrate water bound to Mn_D. The final photooxidation removes an electron from Y_Z-OH, and then according to Sproviero et al. (2008), the tyrosyl radical is reduced by the bound Mn_D-OH^-, giving an Mn_D-$O\cdot^-$ radical whose proton is ejected into the lumen. At this point the Mn_4Ca cluster is in the unstable fully oxidized S_4 state.

Reduction of the Mn_4Ca cluster begins with step 5, in which an O-O peroxy bond is formed by nucleophilic attack of the O(5):$^{2-}$ on the Mn_D-$O\cdot^-$ radical, and transfer of one electron from the -$O\cdot^-$ radical to Mn_D^{4+}. Mn_4Ca reduction is completed in step 6 by formation of the O=O pi bond and transfer of two electrons from the O(5):$^-$ atom, one to Mn_C^{4+} and one to Mn_B^{4+}. The active site is reset in step 7 when an incoming water molecule displaces the bound dioxygen from the O(5) bridging position, becoming deprotonated in the process.

Acknowledgment I wish to thank Holger Dau for his careful reading and helpful comments on this manuscript.

References

Affourtit C, Albury MS, Crichton PG, Moore AL (2002) Exploring the mole-cular nature of alternative oxidase regulation and catalysis. FEBS Lett 510:121–126

Ahlbrink R, Haumann M, Cherepanov D, Bögershausen O, Mulkidjanian A, Junge W (1998) Function of tyrosine Z in water oxidation by photosystem II: electrostatical promotor instead of hydrogen abstractor. Biochem 37(4):1131–1142

Babcock GT (1999) How oxygen is activated and reduced in respiration. Proc Natl Acad Sci U S A 96(23):13114–13117

Babcock GT, Wikstrom M (1992) O_2 activation and the conservation of energy in cell respiration. Nature 356:301–309

Babcock GT, Wikström M (1992) Oxygen activation and the conservation of energy in cell respiration. Nature 356:301–309

Babcock GT, Barry BA, Debus RJ, Hoganson CW, Atamian M, McIntosh L, Sithole I, Yocum CF (1989) Water oxidation in photosystem II: from radical chemistry to multielectron chemistry. Biochem 28:9557–9565

Belevich I, Verkhovsky MI, Wikstrom M (2006) Proton-coupled electron transfer drives the proton pump of cytochrome c oxidase. Nature 440:829–832

Berg JM, Tymoczko JL, Stryer L (2007) Biochemistry, 6th edn., W. H. Freeman, NY; pp. 514–517 and 549–551

Clausen J, Junge W (2004) Detection of an intermediate of photosynthetic water oxidation. Nature 430:480–483

Cook CD, Depatie CB (1959) Oxidation of hindered phenols. VIII. Kinetics of the oxidation of 2,4,6-tri-*t*-butylphenol by benzoyl peroxide. J Org Chem 24:1144–1146

Dau H, Haumann M (2006) Photosynthetic oxygen production: response. Science 312:1471–1472

Dau H, Haumann M (2008) The manganese complex of photosytem II in its reaction cycle—basic framework and possible realization at the atomic level. Coord Chem Rev 252:273–295

De AK, Dutta BK, Bhattacharjee S (2006) Reaction kinetics for the degradation of phenol and chlorinated phenols using Fenton's reagent. Env Program 25:64–71

Haumann M, Liebisch P, Muller C, Barra M, Grabolle M, Dau H (2005) Photosynthetic O_2 formation tracked by time-resolved x-ray experiments. Science 310:1019–1021

Haumann M, Grundmeier A, Zaharieva I, Dau H (2008) Photosynthetic water oxidation at elevated dioxygen partial pressure monitored by time-resolved X-ray absorption measurements. Proc Natl Acad Sci U S A 105(45):17384–17389

Hays A-MA, Vassiliev IR, Golbeck JH, Debus RJ (1998) Role of D1-His190 in proton-coupled electron transfer reactions in photosystem II: a chemical complementation study. Biochem 37:11352–11365

Hoganson CW, Babcock GT (1997) A metalloradical mechanism for the generation of oxygen from water in photosynthesis. Science 277:1953–1956

Hoganson CW, Pressler MA, Proshlyakov DA, Babcock GT (1998) From water to oxygen and back again: mechanistic similarities in the enzymatic redox conversions between water and dioxygen. Biochim Biophys Acta 1365:170–174

Howard DL, Tinoco AD, Brudvig GW, Vrettos JS, Allen BC (2005) Catalytic oxygen evolution by a bioinorganic model of the photosystem II oxygen-evolving complex. J Chem Educ 82:791–794

Joliot P, Kok B (1975) Oxygen evolution in photosynthesis. In: Govindjee (ed) Bio-energetics of photosynthesis. Academic, London, pp 387–411

Kok B, Forbush B, McGloin M (1970) Cooperation of charges in photosynthetic oxygen evolution. I: a linear four-step mechanism. Photochem Photobiol 11:457–475

Mamedov F, Sayre RT, Styring S (1998) Involvement of histidine 190 on the D1 protein in electron/proton transfer reactions on the donor side of photosystem II. Biochem 37:14245–14256

Marechal M, Kido Y, Kita K, Moore AL, Rich PR (2009) Three redox states of *Trypanosoma brucei* alternative oxidase identified by infrared spectroscopy and electrochemistry. J Biol Chem 284:31827–31833

McEvoy JP, Brudvig GW (2004) Structure-based mechanism of photosynthetic water oxidation. Phys Chem Chem Phys 6:4754–4763

Moore AL, Carre JE, Affourtit C, Albury MS, Crichton PG, Kita K, Heathcote P (2008) Compelling EPR evidence that the alternative oxidase is a diiron carboxylate protein. Biochim Biophys Acta 1777:327–330

Pignatello JJ (1992) Dark and photoassisted iron(3+)-catalyzed degradation of chlorophenoxy herbicides by hydrogen peroxide. Environ Sci Tech 26:944–951

Proshlyakov DA, Pressler MA, Babcock GT (1998) Dioxygen activation and bond cleavage by mixed-valence cytochrome *c* oxidase. Proc Natl Acad Sci U S A 95:8020–8025

Rappaport F, Lavergne J (1997) Charge recombination and proton transfer in manganese-depleted photosystem II. Biochemistry 36:15294–15302

Rappaport F, Guergova-Kuras M, Nixon PJ, Diner BA, Lavergne J (2002) Kinetics and pathways of charge recombination in photosystem II. Biochemistry 41:8518–8527

Silverstein TP et al (1993) Transmembrane measurements across bioenergetic membranes. Biochim Biophys Acta 1183:1–3

Sproviero EM, Gascon JA, McEvoy JP, Brudvig GW, Batista VS (2008) Quantum mechanics/molecular mechanics study of the catalytic cycle of water splitting in photosystem II. J Am Chem Soc 130:3428–3442

Svensson-Elk M, Abramson J, Carsson G, Tornoth S, Brzezinski P, Iwata S (2002) The x-ray crystal structures of wild-type and EQ (I-286) mutant cytochrome c oxidases from *Rhodobacter sphaeroides*. J Mol Biol 321:329–339

Tommos C, Babcock G (1998) Oxygen production in nature: a light-driven metalloradical enzyme process. Acc Chem Res 31:18–25

Umena Y, Kawakami K, Shen J-R, Kamiya N (2011) Crystal structure of oxygen-evolving photosystem II at a resolution of 1.9 Å. Nature 473:55–60

Voet D, Voet JG, Pratt CW (2008) Fundamentals of biochemistry, 3rd edn., Wiley, pp. 615–618 and 654–656

Wagner AM, Moore AL (1997) Structure and function of the plant alternative oxidase: its putative role in the oxygen defence mechanism. Biosci Rep 17:319–333

Wikstrom MKF (1977) Proton pump coupled to cytochrome c oxidase in mitochondria. Nature 266:271–273

Wikstrom M, Verkhovsky MI (2006) Towards a mechanism of proton pumping by the haem-copper oxidases. Biochim Biophys Acta 1757:1047–1051

Yano J et al (2006) Where water is oxidized to dioxygen: structure of the photosynthetic Mn_4Ca cluster. Science 314:821–825